The effect of microstructure on the permeability of metallic foams

Medraj, Mamoun; Baril, Éric; Loya, Virendra; Lefebvre, Louis-Philippe

Publisher's version / Version de l'éditeur:
https://doi.org/10.1007/s10853-006-0602-x
Journal of Materials Science, 42, 12, pp. 4372-4383, 2007-03-01

J Mater Sci (2007) 42:4372–4383
DOI 10.1007/s10853-006-0602-x

The effect of microstructure on the permeability of metallic foams

Mamoun Medraj · Eric Baril · Virendra Loya · Louis-Philippe Lefebvre

Received: 28 December 2005 / Accepted: 20 June 2006 / Published online: 1 March 2007

Abstract Pressure drop was measured across complex and simple structure metallic foams at different velocity ranges using air as working fluid. Darcian and non-Darcian permeability parameters, K and C, were determined by fitting experimental data with widely accepted quadratic model of Hazen-Dupuit-Darcy. Generally, the experimental results are in good agreement with the model. The differences in K and C values between the two types of metallic foams are due to the different microstructure. For the simple structure specimens, permeability K increased whereas non-Darcian permeability C decreased with increasing pore diameter. The effect of pore size on the permeability of complex structure metallic foams seems to be opposite to that observed with the simple structure specimens and to results reported by other researchers on other porous medium. This discrepancy mainly stems from the differences in window concentration in addition to some heterogeneity in the foam that impeded the gas flow on one side of the specimens. The difference in pressure drop observed in the different metallic foams is due to combined effect of K and C. However, for simple structure foams, K and C could be predicted by Ergun-like model using appropriate values for the empirical constants. The permeability K is significantly affected by pore size and porosity. The quadratic term of Hazen-Dupuit-Darcy equation is mainly due to the inertia of the flow and partially to the drag exerted by the microstructure of the metallic foam. For both foams, as the porosity increases, pressure drop decreases and permeability, K, increases. The introduction of the open cross sectional area term enabled better understanding of the permeability of metallic foams with intricate morphologies.

M. Medraj (✉) · V. Loya
Mechanical Engineering Department, Concordia University, Montréal, QC, Canada
e-mail: mmedraj@encs.concordia.ca

E. Baril · L.-P. Lefebvre
NRC-IMI, 75 Mortagne, Boucherville, QC, Canada

Introduction

In the last 10 years, various methods for making metallic foams were developed leading to wide ranges of geometries, characteristics and applications. Possible applications for metallic foams range from lightweight construction, sound and heat insulation to energy absorption and medical implants. In many applications such as heat-exchangers, battery electrodes and filters, the resistance to fluid flow through the metallic foam is an important parameter. Control of the flow resistance, characterized by the permeability of the porous media, is important in order to optimize the heat and mass transport in porous media. In addition, permeability of the porous media can be used to integrate the complex geometrical characteristics into a simple formula, and the measurement of permeability could be useful for the characterization of the foam homogeneity.

Flow through porous media was first described by Darcy. Several researchers [1–5] had verified that Darcy's law is valid only for low flow rates where pressure drop is linearly proportional to the flow rate. When velocity increases, the influence of inertia and

turbulence becomes more significant and the pressure drop displays a parabolic trend with velocity. This phenomenon is also known as the non-Darcian flow behavior. As the flow velocity increases, the quadratic term becomes more prevalent and must be accounted for to obtain an accurate description for the pressure drop [6].

Pressure drop across a homogeneous porous medium for steady fluid flow can be described by the Hazen-Dupuit-Darcy model as:

$$\frac{dp}{dx} = \alpha V + \beta V^2 \tag{1}$$

where dx represents the thickness (or length) of the porous medium, dp is the pressure drop across dx, V is the fluid flow velocity, and α and β can be defined as in Eq. 2.

$$\frac{dp}{dx} = \frac{\mu}{K} V + \rho C V^2 \tag{2}$$

where ρ is the fluid density, μ is the fluid viscosity, K is the permeability and C is a coefficient related to the structure of the permeable medium. In Eq. 2, the first term represents the viscous drag and the quadratic term ($\rho C V^2$) accounts for the drag imposed by the solid porous matrix on the flowing media [1]. Flow velocity, V, in Eq. 2 can be either Darcian velocity based on the cross-section dimensions of the channel, $V_D = {}^{Q}/_{area_{CS}}$ or the pore velocity, $V_p = {}^{V_D}/_{\varepsilon}$ where ε is the porosity, as given by the Dupuit-Forchheimer relation [6, 7]. In this work, the velocity based on cross-section dimension, V_D, was used.

Diedericks and Du Plessis [8] showed that the coefficient C becomes more significant as the flow velocity increases. The drag force becomes more prevalent and must be considered for an accurate description of the pressure drop. This drag force compensation may vary according to the porosity of the medium and the channels connecting the pores [9]. Antohe et al. [4] reported that K and C are not flow rate dependant but both coefficients are shown to be velocity range dependent.

Several researchers adopted Ergun-like model to explain and fit their experimental results [10–13]. Bhattacharya and Mahajan [14], for instance, mentioned that Eq. 3 best fit their experimental results.

$$\frac{dp}{dx} = \frac{\mu}{K} V + \rho f \sqrt{K} V^2 \tag{3}$$

where f is the inertial coefficient, also known as Ergun coefficient, K is the permeability, and V is the flow velocity. This model is widely accepted for steady state unidirectional pressure drop in homogeneous, uniform and isotropic porous medium, fully saturated with Newtonian incompressible fluid. K and f are strongly related to the structure of the medium.

In order to optimize the structure and properties of metallic foams for specific applications, it is desirable to be able to predict the permeability as a function of the material's structural characteristics (density, pore size, tortuosity, window size, etc). Although this is difficult to achieve, several attempts [1, 4, 6, 14] have been made to correlate permeability with structural parameters. For instance, Du Plessis [15] and Fourie and Du Plessis [16] modeled metallic foam as a rectangular representative unit cell to predict pressure drop using water and glycerol as working fluids. They stated that their model accurately predicts the pressure gradient in the flow through metallic foam. They reported that inertia coefficient, f, is reduced with increasing porosity. Also, Paek et al. [11] modeled the inertial coefficient, which depends on tortuosity of porous matrix. They expressed that the Du Plessis model is valid only for porosities higher than 97%. Recently, Tadrist and Miscevic [10] adopted Hazen-Dupuit-Darcy model in the form of Eq. 2. They demonstrated that the pressure drop with inertial effects is related to the porosity (ε) and to the average pore diameter (d), using the following equation:

$$\frac{dp}{dx} = A\frac{(1-\varepsilon)^2}{\varepsilon^3 d^2}\mu V + B\frac{(1-\varepsilon)}{\varepsilon^3 d}\rho V^2 \tag{4}$$

where A and B are constants. The major difficulty of using Eq. 4 to evaluate the permeability of complex porous medium, is defining and measuring the structural characteristics. Although the parameter A is clearly quantified for granular media, difficulties arise for metallic foams in which it is assumed that the web-like cellular structure made of solid filaments connected in the three dimensions has a corresponding particle diameter [12]. Tadrist and Miscevic [10] concluded that there is no clear correlation between porosity, ε, and permeability, K, or inertial coefficient, f. Besides, Paek et al. [11] demonstrated that K of a metallic foam increases as the cell size increases for fixed porosity. They further added that pressure drop was minimum at the same solid fraction (1-porosity) for different flow velocities. This indicates that pressure drop depends on cell shape and void fraction.

Other researchers [6, 14, 17] reported experimental and theoretical models between porosity and permeability, demonstrating that permeability increases as porosity increases. In open cell foams, the main bottlenecks to the flow are the windows that connect one

pore to the other. Despois and Mortensen [18] used the similarity between these pores and the porosity network in sintered spherical particles. The permeability of such porous material as a function of the average surface area of the windows between the pores is given by:

$$K = \frac{2(a/\pi)^{3/2}\varepsilon}{\pi\, \mathrm{d}} \tag{5}$$

The average window area (equal to the average contact area at the necks between the two particles) is:

$$a = \frac{\pi}{12}\left(\frac{\varepsilon - \varepsilon_0}{1 - \varepsilon_0}\right)d^2 \tag{6}$$

where ε_o is the initial packing density of the spherical particles (0.64 for the random dense packing of monosized spheres), ε is the solid density in a particle compact (pore volume fraction in the foam) and d is the diameter of the particles. Despois and Mortensen predicted K of open-cell aluminum foams, using Eq. 5. This prediction was done using Darcian flow regime and therefore, the quadratic term was negligible.

Many scientists [2, 6, 19] have correlated the quadratic term to the turbulence of the flow. The permeability based Reynolds number, Eq. 7, has been used to indicate the transition from linear behavior in fully developed steady state to non-linear flow through a porous media.

$$\mathrm{Re}_K = \frac{\rho\sqrt{K}}{\mu}v \tag{7}$$

Antohe et al. [4] argues that using permeability based Reynolds number to indicate transition from linear behavior is a misconception because fully developed steady flow has zero inertia and hence Reynolds number in the form of Eq. 7 has no meaning. Rather, they suggest using the ratio between the form force, D_c, and viscous force, D_μ, as in Eq. 8.

$$\frac{D_c}{D_\mu} = \frac{\rho C V^2}{\frac{\mu}{K}V} \approx \frac{\rho C K}{\mu}V \tag{8}$$

According to Antohe et al. [4], the ratio D_c/D_μ reduces the scattering of data observed when permeable media of very different form are used in hydraulic experiments. Analogous proposals have been put forward recently by Du Plessis et al. [15], Boomsma and Poulikakos [6] and in another study of permeability of ceramic foam by Innocentini et al. [20]. They [6, 15, 20] explained the transition to quadratic behavior, however, they did not agree with Antohe et al. [4] on the issue of inertial effects.

Besides, experimental results obtained by Innocentini et al. [21] showed that the pressure drop versus velocity of gas flow through a membrane is linear in nature, even if the quadratic or inertial term can contribute up to 30% of the overall pressure drop. However, it is not clear from their study that the quadratic contribution to the pressure drop is due to inertia. The transition from linear regime to quadratic regime occurs at a much lower velocity than that corresponding to critical Reynolds number [1]. According to Lage [1], this may be due to a combined effect of inertia, viscosity, form forces and concepts of macroscopic and microscopic domains. He tried to resolve the confusion by giving examples of two different geometries; flow through a straight conduit and a disc like body. Most porous media are a combination of above two geometries and flow through such medium can depart from linear equation to quadratic equation before transition to turbulence [4, 22]. Inertia forces exist at microscopic or at pore level and form forces are macroscopic in nature [4, 22].

Despite the large amount of work done so far to understand the effect of geometrical parameters on the permeability of metal foams, there is no unique relationship that can be drawn. In fact, this could be related to the failure of finding a unique geometrical characteristic that could be then translated into parameters to predict the flow behavior.

The aim of the present work is to categorize various structural parameters responsible for the observed pressure drop across metallic foams, especially to understand the impact of simple and intricate microstructures. The samples studied are very different in nature and permeability. One series of foams is made by metallization of polyurethane foam and the other is produced using a powder metallurgy approach. The former has well distributed and uniform pore structure, while the latter is more tortuous. Experiments were conducted at high velocities of flowing media in order to understand the impact of inertia.

Experimental equipment and procedure

Permeability measurement set up

The experiments were conducted using the instrument shown in Fig. 1. The instrument consists of a middle flange assembly, a pressure transducer, a velocity meter, a pressure vessel and a settling chamber. The instrument was designed to obtain accurate measurements of the flow of compressed air and pressure drop across the specimens. The pressure was controlled

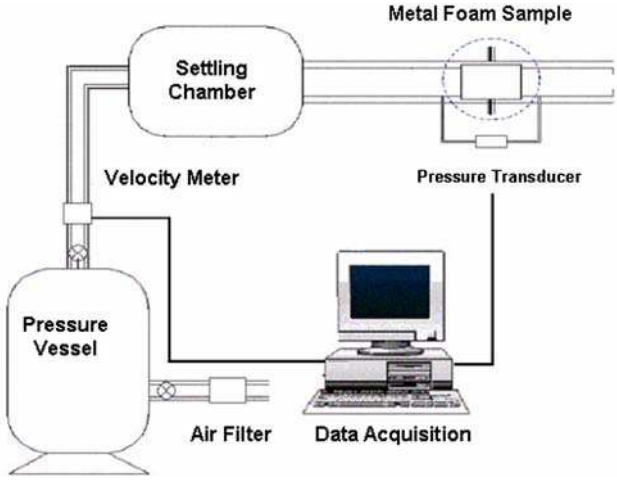

Fig. 1 Experimental set-up

using a manual pressure control-valve. An air filter was employed in line prior to the pressure vessel so that impurities or foreign particles could be removed. Air was then allowed to pass through a settling chamber by means of a 50.8 mm (2-inch) steel pipe. The settling chamber was used to avoid turbulence in the upstream gas flow source. The metallic foam specimens were securely assembled in the middle flange. Pressure taps were drilled on the pipe and one way valves were used to prevent air flow from the holes. The dynamic pressure readings were taken at 5 cm from the metal foams. Downstream pressure was confirmed to be atmospheric pressure by measurement. Upstream pressure was measured using an OMEGA 0–172.4 Pa (0–25 psi) gauge range pressure transducer (±0.1% full scale accuracy). Average flow velocity was measured using an OMEGA 0–20 m/s velocity meter (±1% full scale accuracy). The signals were acquired from the velocity meter and pressure transducer using a data acquisition device connected to a PC. To minimize the error, 100 measurements were collected for each experiment and mean values were used to plot the graphs.

Materials

Simple structure metallic foams (SSMF) were provided by Recemat International, a Netherlands based metal foam manufacturer. They are open cell foams obtained by metallization of a polyurethane foam followed by a thermal decomposition of the polyurethane backbone. This process has good control on the cell size because the polyurethane preforms used have controlled and uniform structures. The detailed process description is given in [23, 24]. Figure 2 shows a typical SSMF microstructure. Nickel-chromium (NC) and nickel-chromium extra strong (NCX) metallic foams with 5 mm, 10 mm and 13 mm thick SSMF samples were tested.

Complex structure metallic foams (CSMF) were made using a powder metallurgy approach at NRC-IMI (Boucherville, Canada). The CSMF's were open-cell nickel foams produced using the method described in [25]. Figure 3 presents a typical microstructure of the foam characterized in this study. The material has a complex network of connecting pores. The microstructure can be roughly defined by the pores (or cells) and the openings between pores (windows).

Density of the foams, measured using the ASTM-792-98 standard is presented in Tables 1 and 2. These porosity data were averaged from three replicas of the same grade. For CSMF, closed porosity was evaluated by means of gas pycnometer using Micromeritics 1305 instrument. The closed porosity is the difference between the apparent and the pycnometer densities.

Pore and window sizes were measured on digitalized SEM micrographs. The pore size was evaluated manually delimiting the pores on the digitalized micrographs and calculating the diameter of circular pores of equivalent area. The window size was determined by drawing the longest lines across the windows to determine the equivalent window diameter and its equivalent projected area (the windows were approximated as circles). Table 2 presents the characteristics of the different complex structure metallic foams. Visual comparison of the microstructure of the two foams in Fig. 2 shows the obvious difference between their respective pore sizes. However, the average window size is not significantly different between the two foams.

Results and discussion

The pressure drop data for the tested metallic foams was normalized per unit length using actual sample thickness (dx). Pressure drop results show that the flow through both SSMF and CSMF open cell metallic foams deviates from Darcy's law and the pressure drop across the foams is a quadratic function of the flow velocity. Equation 1 was used for curve fitting, which is a widely accepted model used by several researchers [11, 12, 14, 17]. The permeability and non-Darcian permeability coefficient were determined for each sample using the entire velocity range of 0–20 m/s by a curve fitting procedure. A least squares fit was performed to determine the values of α and β in Eq. 1. In most cases, the coefficient of determination or square of correlation

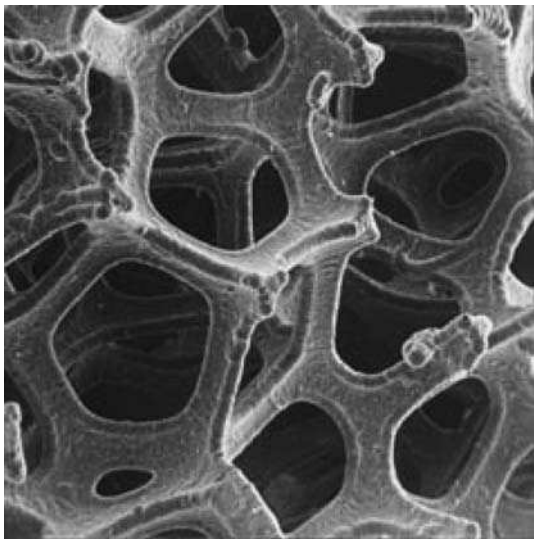

Fig. 2 A typical SSMF microstructure [24]

factor, R^2, is greater than 98%. This indicates that the 2nd order quadratic relationship is valid for all cases. Hence pressure drop can be predicted in the tested velocity range using quadratic equation given by Hazen-Dupuit-Darcy model. Comparing Eqs. 1 and 2, values of K and C were calculated as:

$$K = \frac{\mu}{\alpha}, C = \frac{\beta}{\rho} \tag{9}$$

Dynamic viscosity and density of air used in the calculations are 1.85×10^{-5} pa.s and 1.225 kg/m^3, respectively. Several tests were performed on the same sample to check the repeatability and hysteresis. No hysteresis was noticed and experiments on the same samples were repeatable because the flow was steady, which resulted in unidirectional pressure drop through the specimens. The relative standard deviations (RSD)

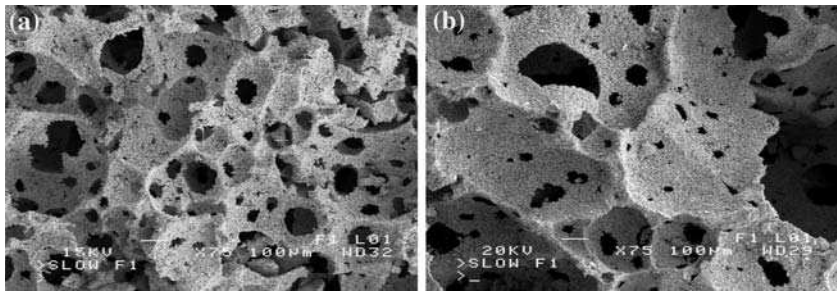

Fig. 3 SEM micrographs at ×75 (**a**) Ni60-1A2 (**b**): Ni70-1A3

Table 1 Structural characteristics of SSMF

Grade, pore diameter	Sample #	Thickness (dx)(mm)	Weight (gm)	V_{foam} (mm^3)	V_{solid} (mm^3)	Volumetric porosity, ε
NC1116-10, d = 1.4 mm	1	10.01	8.5	17,377	1,647	0.91
	2	10.00	8.7	17,356	1,686	0.90
	3	10.40	11.0	18,051	2,131	0.88
NC1116-13, d = 1.4 mm	1	13.23	15.4	22,966	2,984	0.87
	2	13.27	13.1	23,035	2,538	0.89
	3	13.24	12.9	22,980	2,500	0.89
NCX1723-10, d = 0.9 mm Extra Strong	1	10.17	9.4	17,648	1,821	0.90
	2	10.40	11.1	18,051	2,151	0.88
	3	10.23	10.3	17,759	1,996	0.89
NC2733-5, d = 0.6 mm	1	4.87	4.6	8,456	891	0.89
	2	5.10	4.7	8,859	910	0.90
	3	4.90	4.4	8,512	852	0.90
NC2733-10, d = 0.6 mm	1	10.00	10.0	17,363	1,937	0.89
	2	10.20	9.4	17,704	1,821	0.90
	3	10.20	9.9	17,704	1,918	0.89
NCX2733-10, d = 0.6 mm Extra Strong	1	10.34	14.0	17,953	2,713	0.85
	2	10.40	14.7	18,051	2,848	0.84
	3	10.23	14.7	17,752	2,848	0.84
NC3743-5, d = 0.5 mm	1	5.16	7.8	8,956	1,511	0.83
	2	5.20	7.7	9,025	1,492	0.84
	3	5.10	7.6	8,852	1,472	0.83
NC4753-5, d = 0.4 mm	1	5.30	6.0	9,206	1,162	0.87
	2	5.31	6.3	9,220	1,220	0.87
	3	5.30	7.1	9,206	1,375	0.85

Table 2 Structural characteristics of CSMF

Sample	Thickness (mm)	Volumetric porosity			Pore diameter (μm)		Window diameter (μm)	
		Total	Open	Standard deviation	Average	Standard deviation	Average	Standard deviation
Ni70-1A3	11.85	0.92	0.90	0.0005	485.7	17.35	57.0	2.42
Ni70-1A4	11.40	0.92	0.90	0.0004	461.5	26.39	57.2	2.38
Ni70-1A5	11.40	0.92	0.90	0.0002	512.4	19.93	55.4	2.17
Ni60-1A2	8.38	0.94	0.93	0.0008	307.6	21.41	54.0	3.52
Ni60-1A3	8.96	0.94	0.91	0.0022	309.8	29.86	67.9	0.44
Ni60-1A4	8.27	0.95	0.92	0.0006	273.2	24.34	56.3	1.32

of the measurements were 1.89% and 1.74% for K and C values, respectively. The repeatability of the measurements was also evaluated by performing the experiment on 3 replicas for each foam. This provided the average and standard deviations of K and C measurements within the same grade of foams. The RSD of the 3 replicas of the same foam geometry were between 7.5 and 26% for both K and C. Hence the variation from one sample to another is much larger than the RSD of the permeability measurement. This was taken into account in the analysis of the results. Several publications [4, 6, 26] presented theoretical uncertainty analyses for the measurement of K and C using a similar experimental and curve fitting approach to the one reported in this paper. They reported relative uncertainties in the range of 3.1–13.9% and 7.9–15.2% for K and C, respectively. These are much larger than the RSD of the permeability measurements of this study but close to the RSD observed within the replicas.

Simple structure metallic foams

For various SSMF specimens, pressure drop was measured at different velocities as can be seen in Fig. 4. These results were obtained by averaging the values of the three replicas of each grade. It can be seen that as the pore size increases, pressure drop decreases.

Figure 5 presents K and C values for the SSMF's versus pore diameter. It can be seen from this figure that K increases and C decreases when the pore size increases. This indicates that K and C are highly correlated with pore diameter for these foams.

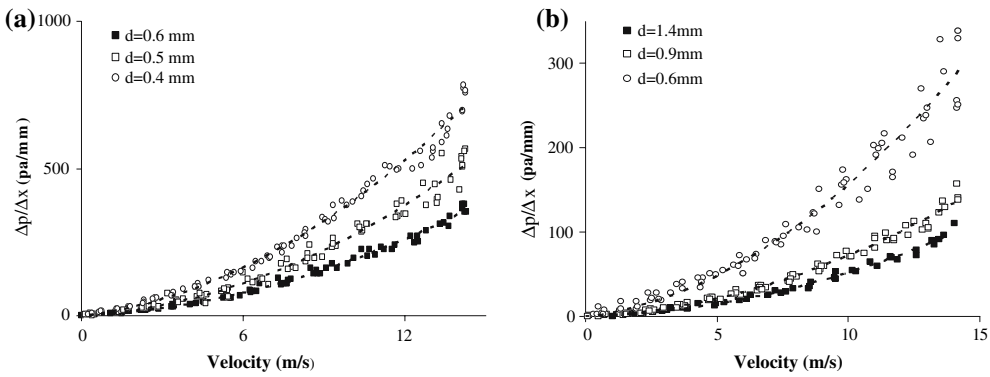

Fig. 4 Pressure drop per unit length versus velocity for (**a**) 5 mm and (**b**) 10 mm thick SSMF

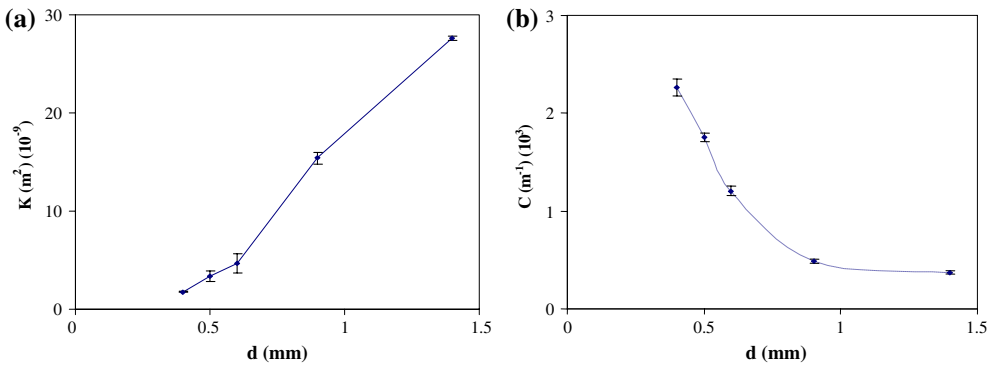

Fig. 5 Permeability versus pore diameter for SSMF; (**a**) K and (**b**) C

The effect of thickness on the permeability of metallic foam was also observed. For the same pore diameter (d = 0.6 mm) SSMF, 5 mm and 10 mm thick samples showed similar values of K (4.70×10^{-9} and 4.93×10^{-9} m^2). The thickness of the SSMF has marginal effect on K and C. This is probably due to the uniform morphology of the SSMF over the length.

For large pore samples (d = 1.4 mm, dx = 13 mm), coefficient α in Eq. 1 was negative. When α was set to zero (i.e. K is infinity), the quadratic part of the equation predicted the experimental pressure drop well; indicating that pressure drop in large pore SSMF was mainly due to drag force and/or inertial effect of the flowing fluid. Fitting the data with a 3rd order polynomial slightly improves R^2 value, but 2nd order curve was selected for calculating the K and C because it is more scientifically based.

Figure 6 illustrates the relation between K and C and velocity ranges for 5 mm thick SSMF. For the whole velocity range (0–15 m/s), velocity had no significant effect on K. However, standard deviations in the measurements of K were higher in the high velocity range (8–15 m/s). This may be due to variations in the morphology between the three replicas of the same foam and the effect of these variations on permeability in the higher velocity range. The standard deviations in the measurements of C were comparatively lower. Similar trends were observed for the 10 mm SSMF samples. Also, it was observed that for larger pore diameter (d = 1.4 mm), C varies significantly in the high velocity ranges.

Figure 7 shows K and C versus porosity. Apparently, K shows no clear trend with porosity; within the interval of porosity studied. The value of K for a porosity of 0.90 and pore size of 1.4 mm is 2.8×10^{-8} m^2, which is in the same order of magnitude as value reported by Bhattacharya (5.3×10^{-8} m^2) [10] for an aluminum foam with similar characteristics (i.e. d = 1.8 and porosity = 0.9132).

Figure 8 shows that the pressure drop contribution from the quadratic term of Eq. 1 is large compared to the Darcian velocity term. For pore diameter 1.4 mm, this contribution is more than 80 % of the total pressure drop. As the pore size increases, the contribution of the quadratic term to pressure drop increases. This suggests that this contribution is predominant not only at high velocity, but for large pore diameter as well.

Figure 9 shows a comparison between experimental and calculated (using Eq. 4) K and C values for the

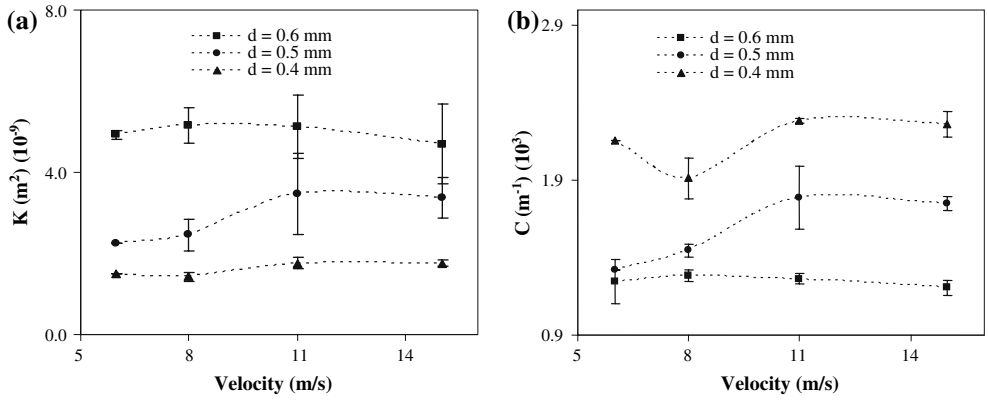

Fig. 6 Permeability at different velocities for 5 mm thick SSMF; (**a**) K and (**b**) C

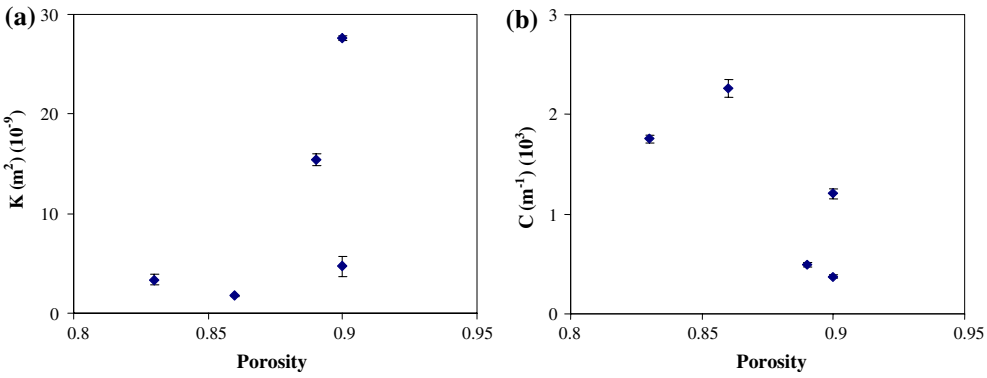

Fig. 7 (**a**) K and (**b**) C versus porosity for various SSMF

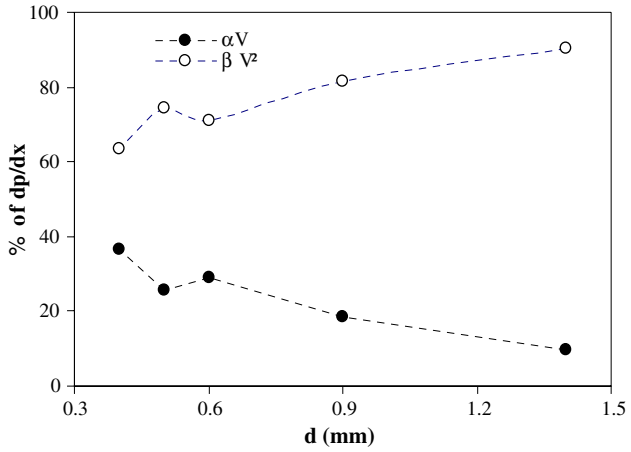

Fig. 8 Pressure drop contribution from the two terms of Eq. 1 (SSMF foams)

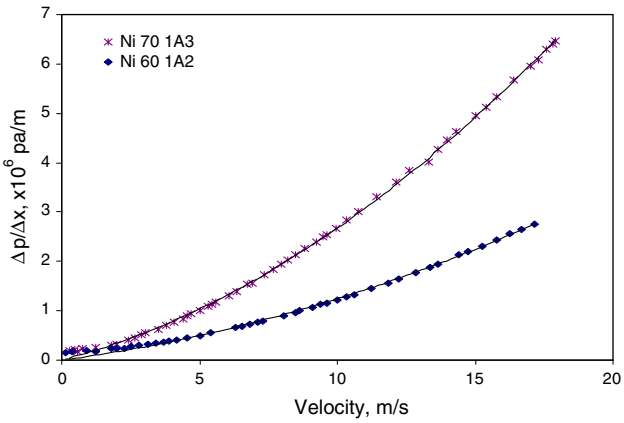

Fig. 10 Unit pressure drop versus velocity for Ni70-1A3 and Ni60-1A2 samples

simple structure metallic foams with different pore diameters. It can be seen that K increases with the average pore diameter. Values of A and B used in Eq. 4 were 100 and 1.0, respectively. These values lie within the intervals obtained by Tadrist and Miscevic [10]; from 100 to 865 for constant A and 0.65 to 2.65 for constant B, obtained by testing various kinds of porous structures. Experimental results of the SSMF are in agreement with the model suggested by Tadrist and Miscevic. This model is Ergun-like model, which is derived from the Hanzen-Dupuit-Darcy equation.

Complex structure metallic foam

The CSMF samples were available in two different morphologies. Figure 10 shows the unit pressure drop measured against velocities for Ni70-1A3 and Ni60-1A2. Pressure drop for all the Ni70 samples was found to be much higher than for the Ni60 samples, although the average pore diameter for Ni60 is smaller than that of Ni70. An attempt to explain this observation will be given in this section.

K and C of both Ni70 and Ni60 CSMF calculated for different velocity ranges are presented in Fig. 11. It can be seen that K and C values are relatively constant within the velocity range used in this study. In addition, the values of K are much lower for CSMF than SSMF while C values are much higher for CSMF than SSMF. Higher K values for Ni60 samples are observed but the differences between Ni60 and Ni70 are not significant in the lower velocity ranges. On the other hand, the coefficient C is much higher for Ni70 than for Ni60. However, it should be noticed that the relative contribution of the quadratic term of Eq. 2 on the normalized pressure drop is identical for both CSMF (see Fig. 12). Therefore, the difference in pressure drop between Ni60 and Ni70 is related to differences in both the viscous drag and the drag imposed by the solid porous matrix and it is not dominated by one or the other.

Through image analysis, pore sizes and window sizes were measured. The average pore size for Ni70 and Ni60 was 486 ± 26 μm and 296 ± 23 μm, respectively. Visual comparison of the SEM pictures of the two different foams (Fig. 3) shows the obvious difference between the pore sizes. However, the average window size for Ni70 and Ni60 was 56.5 ± 2.3 μm and

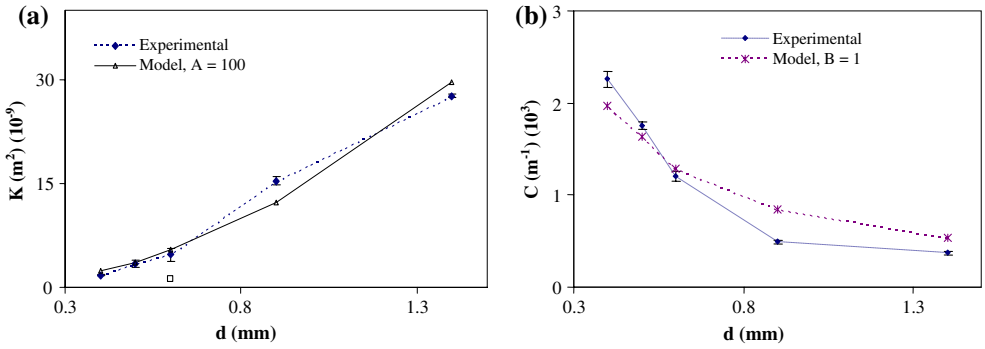

Fig. 9 Model (Eq. 4) versus experimental results for (**a**) permeability coefficient and (**b**) non-Darcian coefficient (SSMF foams)

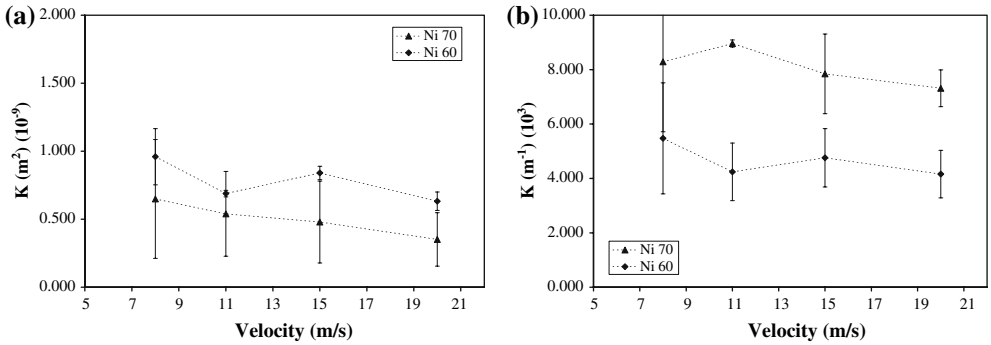

Fig. 11 (**a**) K and (**b**) C versus velocity for Ni70 and Ni60 CSMF samples

59.4 ± 1.8 μm, respectively. There is not much difference between the windows size for the two different foams.

Figure 13 demonstrates that pressure drop was lower for smaller pore diameter. This is contrary to what is generally expected. However, from the micrographs in Fig. 3, it can be seen that the number of pores in a given area is much lower for Ni70 compared to Ni60. This implies that the open area for the flow of air through a particular section is larger for Ni60 compared to Ni70 samples. This reveals the main cause behind the lower pressure drop measured on the Ni60 foams.

This particular outcome was investigated further with sectioning the thickness of the metallic foams. Foam samples were machined in steps by removing layers of 0.5–1.5 mm thickness. Samples were cleaned after machining using compressed air to ensure that no dust was left in the pores. After each sectioning step, pressure drop and microstructure data were collected. Pressure drop for various thicknesses of Ni70-1A4 and Ni70-1A3 samples are given in Fig. 14a and b, respectively. From these figures, it is evident that the unit pressure drop is not constant across the thicknesses. This is more noticeable in Fig. 14b for Ni70-1A4 sample. However, in Fig. 14a showing the Ni70-1A4 results, pressure drop data lie on the same quadratic curve, excepted for thickness 11.4 mm. Whereas for Ni70-1A3 (Fig. 14b), separate quadratic curves could be seen for most of the thicknesses. This suggests that the structure of the layers machined off were different from the rest of the whole specimens (assuming that the machining did not modify the pore opening on the surface). Figure 15, which presents the pressure drop recorded at different thicknesses for various CSMF samples, suggest that this is the case since a correlation exists between the pressure drop and the thickness. The source of this inhomogeneity in the Ni70 should come from the partial collapse of the bottom of the foams during foaming. The viscosity of the suspension was probably not high enough to stabilize the foam during foaming causing a partial collapse of the foam and the closure of some porosity on one side of the foam. This effect could in fact be observed visually on the Ni70 foams.

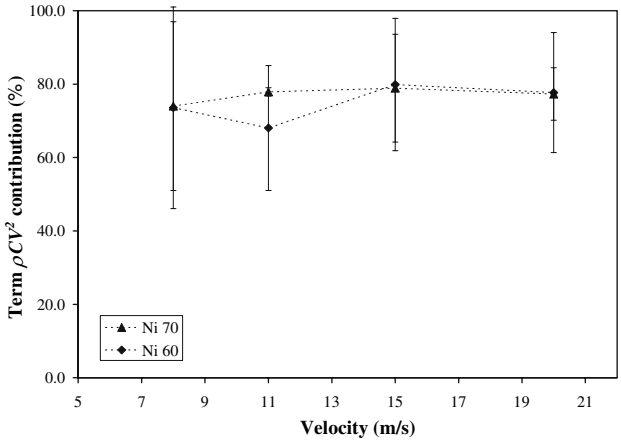

Fig. 12 Effect of the fluid velocity on the relative contribution of the term ρCV^2 of Eq. 2 on the normalized pressure drop ($-\Delta P/\Delta x$) for CSMF samples

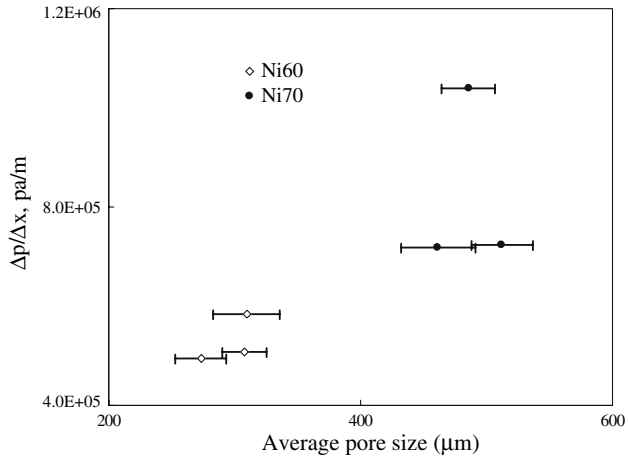

Fig. 13 Pressure gradient ($\Delta P/\Delta x$) measured at 5 m/s as function of the average pore size (CSMF foams)

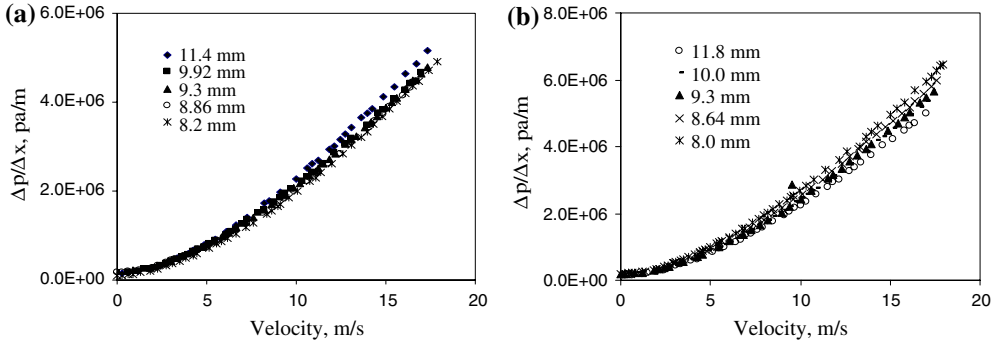

Fig. 14 Unit pressure drop versus velocity for various thicknesses of (**a**) Ni70-1A4 and (**b**) Ni70-1A3

Figure 15 shows that linear relation could be drawn for Ni70 samples, suggesting that the layers removed had similar microstructures. The regression lines do not pass through zero because the structure of those layers is different from that of the whole specimens. Besides, the slope of the line of Ni70-1A3 sample is different from the slopes of the Ni70-1A4 and Ni70-1A5 lines, probably because sample Ni70-1A3 was machined on the surface having the highest porosity while specimens Ni70-1A4 and Ni70-1A5 were machined on the low permeability side.

Reasons behind this ambiguity could be investigated by interpreting pressure drop for each layer. Factors that are affecting pressure drop for each individual layer were studied. Hence, each layer machined, was analyzed as one sample. Therefore, microstructure of the individual layers could be studied in greater detail. Pictures of the surface of the CSMF were taken at five different zones. Open area for the flow of air was measured for all these individual zones and then added. These readings are given in Table 3. Pressure drop for the particular layer is calculated by means of mathematical subtraction of the pressure drop before and after machining.

From Fig. 16, it is apparent that as the open area to the flow of air through the metallic foam layer increases, the pressure difference across that layer decreases. Although, the pore diameter in Ni70 is greater than in Ni60, the open area is smaller and this causes larger pressure drop across the foam thickness. The wall of the pores creates resistance to the flow of air and hence it is clearer that the pressure drop does not

Table 3 Pressure drop, open area to the flow of air and thickness of individual layers

Sample	Pressure drop (pa)	Open area (μm^2)	Thickness (mm)
Ni 70-1A5	508.93	725039.8	0.70
Ni 70-1A3-4	390.00	675991	0.66
Ni 70-1A4-4	720.93	450280	0.54
Ni 70-1A3-5	169.17	869758.2	0.64
Ni 70-1A4-5	994.3	367869.9	0.56
Ni60-1A3	310.08	1217415	0.55
Ni60-1A4	105.52	945122.6	0.52

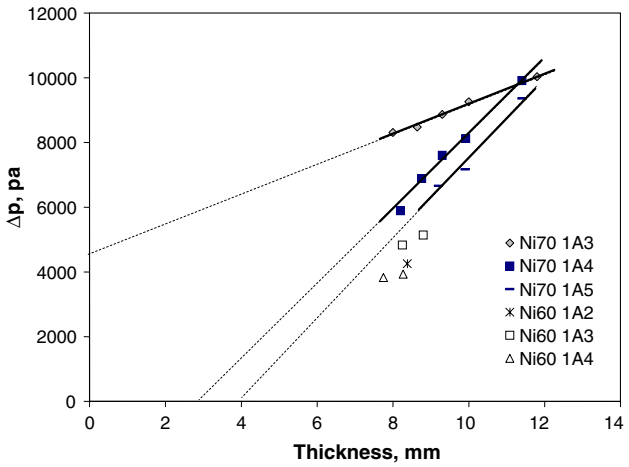

Fig. 15 Pressure drop for the CSMF samples with different thicknesses at 5 m/s

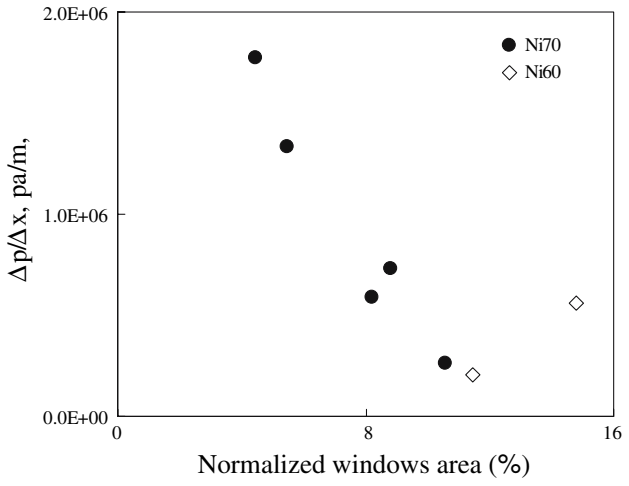

Fig. 16 Unit pressure drop measured at 5 m/s as a function of normalized window area (the total area of the windows divided by the examined area 8.24 mm^2)

depend only on the pore size or porosity of complex structure metallic foam.

In another test, composite of two discs of Ni70-1A3 and Ni60-1A4 was prepared. Pressure drop data was collected at various velocities for two different scenarios through alternating the orders of the discs. In the first case, Ni60-1A4 disc was facing the flow and in the second Ni70-1A3 disc was facing the flow. The results of this test are shown in Fig. 17.

Figure 17 shows that alternating the order of the discs did not affect the pressure drop behavior of the composite foam. While, by mathematically adding the pressure drop for each disc tested individually, higher pressure drop resulted. This difference is quite noticeable and is an evidence of pressure drop due to inertia. When air impacts the surface of the metallic foam, there is a sudden change in momentum causing a pressure loss. When the pressure drop is added mathematically, this loss was counted two times. While in the composite case, the pressure drop due to a sudden impact was counted only once. This indicates that the quadratic term of the Hazen-Depuit-Darcy equation is mainly due to the inertia of the flow and partially to the drag exerted by the microstructure of the metallic foam.

From the porosity measurements, the average porosities for the three replicas of Ni60 and Ni70 are 94.2% and 92%, respectively. This means that the volume fraction of the voids in Ni60 is higher than in Ni70. Figure 18 represents porosity versus unit pressure drop at 5 m/s for various CSMF's. As the porosity decreases, the unit pressure drop increases and the permeability decreases.

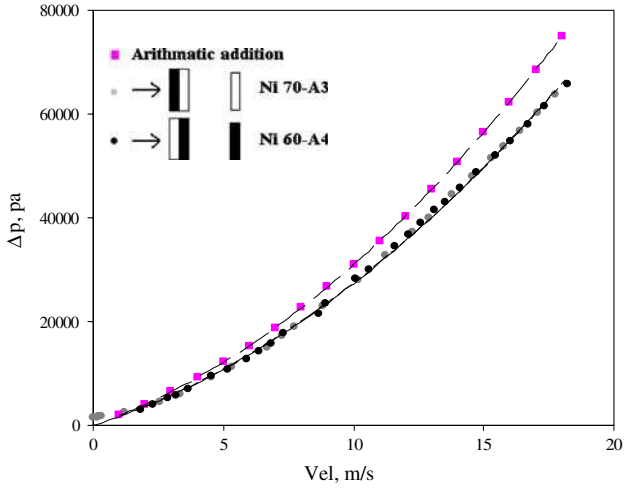

Fig. 17 Pressure drop versus velocity for the composite CSMF discs

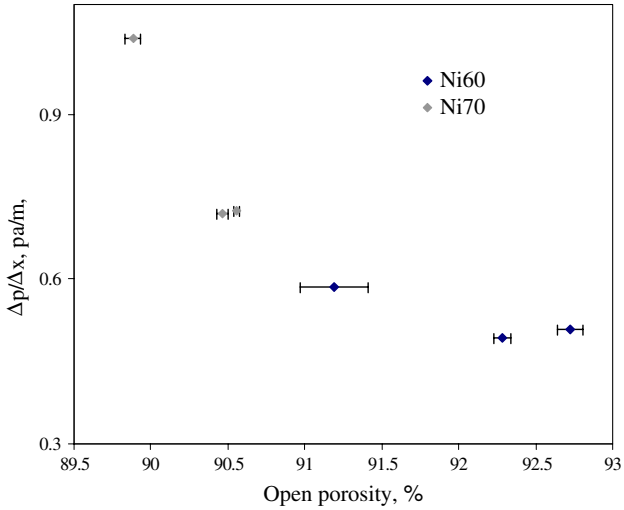

Fig. 18 Unit pressure drop versus porosity at 5 m/s

Permeability of the SSMF and CSMF samples were also compared with the model suggested by Despois and Mortensen [18]. Figure 19 shows the combined effect of pore size and porosity on the permeability and a comparison with Despois and Mortensen model. The model predicts the general trend for both SSMF and CSMF but higher values than those of CSMF and lower than those of SSMF samples. This suggests that there are other morphological parameters which need to be included for an accurate prediction of the permeability. Moreover, Despois and Mortensen assumed that there is one active window per pore, an assumption that is not true for the foams studied in this study. More importantly, this model is valid only for the Darcian velocity range, conditions that were not maintained in the present study.

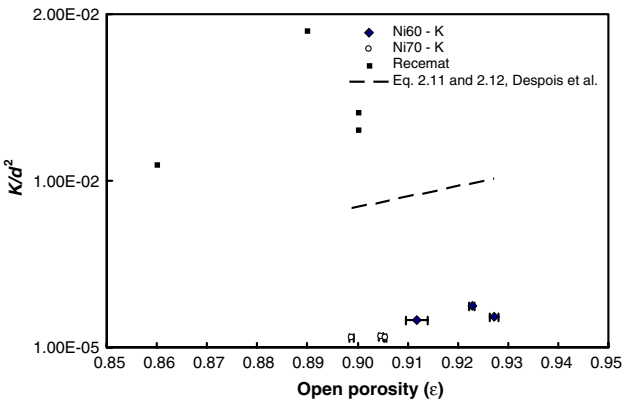

Fig. 19 Effects of the foam porosity on the permeability (K) normalized by the pore size squared (d^2) compared to the model of Despois and Mortensen [18]

Conclusions

The main conclusions that can be drawn from the present work are:

(i) Pressure drop characteristics of both the simple and complex structure metallic foams were found to fit the polynomial model of Hazen-Depuit-Darcy.

(ii) For the experimental conditions evaluated, the pressure drop observed in the metallic foams is due to a combined effect of K (permeability) and C (non-Darcian permeability co-efficient).

(iii) The differences in K and C values between the two types of metallic foams result from the differences in the microstructure of the foams.

(iv) For SSMF specimens, permeability K increased whereas non-Darcian permeability C decreased with increasing pore diameter.

(v) The effect of pore size on the permeability of CSMF seems to be opposite to that observed with the SSMF specimens and for other porous medium reported by other researchers. This may be due to window concentrations that were significantly larger for the specimens having the smaller pores and some heterogeneity in the foam having the larger pores, which could impede the gas flow on one side of the specimens.

(vi) For the CSMF, open cross sectional area for the flow of air is found to be the critical factor for the pressure drop behavior and the combination of window size and numbers of windows have to be considered for predicting the pressure drop.

(vii) The behavior of fluid flow in porous medium can be very complex. However, K and C could be predicted by Ergun-like model for the SSMF using appropriate A and B constants.

Acknowledgement The authors gratefully acknowledge the financial support received from NSERC and NATEQ. The authors would also like to thank NRC-IMI, Boucherville, Quebec, Canada and RECEMAT International, Netherlands for providing the samples.

References

1. Lage JL (1998) In: Ingham BD, Pop I (eds) Transport phenomena in porous media. pp 1–30
2. Ward JC (1964) ASCE J Hydraulics Division 90(HY5):1
3. Beavers GS, Sparrow EM, Rodenz DE (1973) J Appl Mech 40(3):655
4. Antohe BV, Lage JL, Price DC, Weber RM (1997) J Fluids Eng 119(2):405
5. Davis PA, Olague NE, Goodrich MT (1992) Adv Water Resour 15:175
6. Boomsma K, Poulikakos D (2002) J Fluids Eng 124(1):263
7. Scheidegger AE (1974) The physics of flow through porous media. 3rd edn., University of Toronto Press, ISBN: 0-8020-1849-1
8. Diedericks GPJ, Du Plessis JP (1997) Math Eng Industry 6(3):133
9. Beckermann C, Viskanta R (1987) Int J Heat Mass Transfer 30(7):1547
10. Tadrist L, Miscevic M (2004) Exp Thermal Fluid Sci 28(2):193
11. Paek JW, Kang BH, Kim SY, Hyun JM (2000) Int J Thermophys 21(2):453
12. Innocentini DM, Salvini Vania (1999) Mater Res (Sao Carlos, Brazil) 2(4):283
13. Innocentini DM, Victor C (2001) J Am Ceramic Soc 84(5):941
14. Bhattacharya A, Mahajan RL (2002) Int J Heat Mass Transfer 45(5):1017
15. Du Plessis P (1994) Chem Eng Sci 49(21):3545
16. Fourie JG, Du Plessis P (2002) Chem Eng Sci 57(14):2781
17. Boomsma K, Poulikakos D, Ventikos Y (2003) Int J Heat Fluid Flow 24(6):825
18. Despois JF, Mortensen A (2005) Acta Materialia 53(5):1381
19. Fand RM, Kim BYK, Lam ACC, Phan RT (1987) ASME J Fluids Eng 109(3):268
20. Innocentini DM, Salvini VR, Pandolfelli VC, Coury JR (1999) Am Ceramic Soc Bull 78(9):78
21. Innocentini DM, Antunes WL, Baumgartner JB, Seville JPK, Coury JR (1999) Mater Sci Forum 299–300(5):19
22. Rumer RR, Drinker P (1966) J Hydraulic Div., Am Soc Civil Engineers 89(6):193
23. Banhart J, Baumeister J (1998) J Mater Sci 33(6):1431
24. ReceMat International, ''RECEMAT® metal foam: extremely porous material'', http://www.recemat.com/en/, on 28th December, 2005
25. Gauthier M, Lefebvre L, Thomas Y, Bureau M (2004) Mater Manufact Process 19(5):793
26. Dukhan N, Alvarez A, (2004) In: Proceedings of the 2004 ASME international mechanical engineering congress and exposition, Anaheim, California USA, November 13–20 pp 595–601